2021 American Control Conference (ACC)
New Orleans, USA, May 25-28, 2021

Unified Position and Attitude Control of A Fully Nonlinear Quadrotor*

Boyang Zhang[1] and Henri P. Gavin[1]

Abstract— **This paper presents a departure from hierarchical cascade methods to control the position and attitude of a fully nonlinear quadrotor. The paper presents a nonlinear feedback control scheme that simultaneously controls position and attitude. The proposed method is based on a generalization of the Gauss's Principle of Least Constraint (GPLC) for higher-order constrained dynamical systems. By double differentiating the rigid-body position dynamics of a fully nonlinear quadrotor with respect to time, the translational and rotational dynamics become fully coupled at the levels of snap and angular acceleration, and the quadrotor is turned into a fully actuated system in a reduced configuration space. A generalized Baumgarte's error stabilization (BES) is developed to asymptotically drive constraint errors to zero. The nonlinear control law is due purely to the natural evolution of constrained system dynamics. To the best of our knowledge, this is the first instance that GPLC and BES are both extended to higher-order systems and that the control scheme for the position and attitude of a quadrotor is unified into one step by making use of its fully nonlinear constrained dynamics. The efficiency and efficacy of the proposed method is demonstrated by numerical experiments on a quadrotor tracking a prescribed conical spiral.**

I. INTRODUCTION

Quadrotors are gaining an increasing interest in many applications due to their design simplicity and agile maneuverability [1]. Quadrotors are inherently challenging to control since they are nonlinear, underactuated, and have limited energy storage. In 2019, Nascimento and Saska [2] reviewed over 800 papers on multi-rotor aerial vehicle (MAV) control and concluded that the predominant literature on MAV control is based on system and control theory that makes use of a cascade control framework, in which the inner loop attitude controller responses much faster than the outer loop position controller. Further, approximately half of the work employ linearized vehicle dynamics in controller synthesis [2]. Cascade position-attitude control does not account for the true inherent coupling of the quadrotor's translational-rotational dynamics. Furthermore, the performance of cascade control architectures may not be sufficiently robust to the unavoidable issues of constraint violations that may arise from actuator delays, model uncertainties, or exogenous disturbances. In addition, aggressive flights in obstacle-rich environments may be difficult for control methods based on linearized vehicle dynamics.

Few work has been conducted on unifying the position and attitude controllers for quadrotors. These unified position-attitude control methods include linear proportional-integral-derivative control [3], nonlinear model predictive control [4], and sequential linear quadratic control [5], [6]. Having merits of their own, these methods, however, adopt partially linearized [3], [4] or fully linearized [5], [6] vehicle dynamics in controller synthesis and requires iterative solution of an optimization problem [4], [5], [6] that has no global optimum guarantee [5], [6]. Moreover, the required number of the control parameters is relatively large whose physical meanings are in general challenging to be interpreted [3], [4], [5], [6].

Udwadia and Kalaba (U-K) [7] rejuvenated Gauss's Principle of Least Constraint (GPLC) [8] by proposing U-K equations, which have been used to analytically solve problems of constrained mechanical systems [9], [10]. U-K controls are applicable only to systems with second-order dynamics, in which relative contributions of each constraint to the net control actions may not be distinguished from each other due to the elimination of Lagrange multipliers.

In this paper, we extend GPLC for a higher-order constrained dynamical system and express its dynamics as a Karush-Kuhn-Tucker (KKT) system to address the limitations of the U-K approach. The *generalized* GPLC (GGPLC) is used to synthesize a unified position-attitude controller for a fully nonlinear quadrotor. To the best of our knowledge, this is the first instance that generalizes GPLC and uses it in the control of any system and that unifies the position and attitude control of a quadrotor without linearizing the quadrotor's fully nonlinear dynamics at any stage. The proposed unified control architecture only involves the solution of a matrix equation, without iteration, at each time step and ensures the global optimality of the solution. The control parameters in our method are physically interpretable with a number of which less than that of the existing unified control approaches. A generalized constraint error stabilization is also developed to asymptotically drive the tracking constraint errors to zero.

This paper is organized as follows. In Section II, we lay out the foundations for the GGPLC for controlling higher-order nonlinear dynamical systems. Then in Section III, we formulate the unified position-attitude control of a quadrotor based on its fully nonlinear dynamics. Next, numerical results and discussions are presented in Section IV, followed by the contributions and future work in Section V.

II. CONTROL OF HIGHER-ORDER CONSTRAINED DYNAMICAL SYSTEMS

A. GPLC (Second-Order Systems)

Consider a system of N second-order ordinary differential equations (ODEs), describing, for example, the accelerations

*This work was supported in part by the U.S. Army Research Office under award number 75568-NS-II.

[1]B. Zhang and [1]H.P. Gavin are with Department of Civil and Environmental Engineering, Duke University, Durham, NC, 27708 USA boyang.zhang@duke.edu, henri.gavin@duke.edu.

2021 American Control Conference (ACC) | 978-1-6654-4197-1/21/$31.00 ©2021 IEEE | DOI: 10.23919/ACC50511.2021.9483358

of an unconstrained dynamical system in terms of N generalized coordinates $\mathbf{q}(t)$, $\mathbf{M}(\mathbf{q},t)\,\mathbf{a} = \mathbf{f}_{\rm nc}(\mathbf{q},\dot{\mathbf{q}},t)$, where $\mathbf{M} \in \mathbb{R}^{N\times N}$ is a matrix of mass and inertial properties, $\mathbf{a}$ denotes unconstrained accelerations, and $\mathbf{f}_{\rm nc} \in \mathbb{R}^N$ contains all nonconstraint (noncontrol) forces exerted on the system. We note here that in the absence of constraints, $\mathbf{a} = \ddot{\mathbf{q}} \in \mathbb{R}^N$, and that elements of $\ddot{\mathbf{q}}$ are the highest-order derivatives in each equation.

A doubly-differentiable constraint on positions $g_j(\mathbf{q},t) = 0$ raised to the acceleration level is linear in accelerations,

$$\ddot{g}_j = \dot{\mathbf{q}}^{\mathsf{T}}\left[\frac{\partial^2 g_j}{\partial \mathbf{q}^2}\right]\dot{\mathbf{q}} + \frac{\partial g_j}{\partial \mathbf{q}}\ddot{\mathbf{q}} + \frac{\partial^2 g_j}{\partial t^2} = 0\ ,$$

and a system of such differentiated constraints g_j, $j = 1,2,\ldots,C$, is expressed herein as $\mathbf{A}(\mathbf{q},t)\,\ddot{\mathbf{q}} = \mathbf{b}(\mathbf{q},\dot{\mathbf{q}},t)$ with initial conditions $\mathbf{g} = \mathbf{0}$ and $\dot{\mathbf{g}} = \mathbf{0}$ at $t = 0$, where $\mathbf{A} \in \mathbb{R}^{C\times N}$ is the Jacobian matrix of $\mathbf{g}$ with respect to $\mathbf{q}$. GPLC [8] states that constrained accelerations $\ddot{\mathbf{q}}$ minimize the quadratic form of the difference between the constrained accelerations $\ddot{\mathbf{q}}$ and the unconstrained accelerations $\mathbf{a}$. This principle may be deduced by recognizing that $\mathbf{M}\ddot{\mathbf{q}} = \mathbf{f}_{\rm nc}$ solves

$$\min_{\ddot{\mathbf{q}}} \frac{1}{2}\ddot{\mathbf{q}}^{\mathsf{T}}\mathbf{M}\ddot{\mathbf{q}} - \ddot{\mathbf{q}}^{\mathsf{T}}\mathbf{f}_{\rm nc}\ ,$$

and that constraining the minimization to satisfy $\mathbf{A}\ddot{\mathbf{q}} = \mathbf{b}$ is

$$\max_{\boldsymbol{\lambda}}\min_{\ddot{\mathbf{q}}} \frac{1}{2}\ddot{\mathbf{q}}^{\mathsf{T}}\mathbf{M}\ddot{\mathbf{q}} - \ddot{\mathbf{q}}^{\mathsf{T}}\mathbf{f}_{\rm nc} + \boldsymbol{\lambda}^{\mathsf{T}}(\mathbf{A}\ddot{\mathbf{q}} - \mathbf{b})\ , \tag{1}$$

which is equivalent to [11]

$$\max_{\boldsymbol{\lambda}}\min_{\ddot{\mathbf{q}}} \frac{1}{2}(\ddot{\mathbf{q}} - \mathbf{a})^{\mathsf{T}}\mathbf{M}(\ddot{\mathbf{q}} - \mathbf{a}) + \boldsymbol{\lambda}^{\mathsf{T}}(\mathbf{A}\ddot{\mathbf{q}} - \mathbf{b})\ , \tag{2}$$

by noting that $\ddot{\mathbf{q}}^{\mathsf{T}}\mathbf{f}_{\rm nc} = \ddot{\mathbf{q}}^{\mathsf{T}}\mathbf{M}\mathbf{a}$ and that $\mathbf{a}^{\mathsf{T}}\mathbf{M}\mathbf{a}$ is a constant in terms of solving the constrained optimization (2). We call (1) the GPLC, which is an equivalence of the *original* GPLC (2). The solution to (1) is represented by the KKT system

$$\begin{bmatrix}\mathbf{M} & \mathbf{A}^{\mathsf{T}}\\ \mathbf{A} & \mathbf{0}\end{bmatrix}\begin{bmatrix}\ddot{\mathbf{q}}\\ \boldsymbol{\lambda}\end{bmatrix} = \begin{bmatrix}\mathbf{f}_{\rm nc}\\ \mathbf{b}\end{bmatrix}\ , \tag{3}$$

where $\mathbf{0}$ denotes a zero matrix of compatible dimensions. The KKT system (3) represents the constrained equations of motion in which the constraint forces are $\mathbf{f}_{\rm c} \triangleq -\mathbf{A}^{\mathsf{T}}\boldsymbol{\lambda}$. Section II-C provides the sufficient and necessary conditions for a unique solution to (3).

The constrained acceleration $\ddot{\mathbf{q}}$ and the constraint forces $\mathbf{f}_{\rm c}$ for the constrained dynamics problem (1) can be also calculated by

$$\begin{aligned}\ddot{\mathbf{q}} &= \mathbf{a} + \mathbf{M}^{-1}\mathbf{K}(\mathbf{b} - \mathbf{A}\mathbf{a})\,,\\ \mathbf{f}_{\rm c} &= \mathbf{K}(\mathbf{b} - \mathbf{A}\mathbf{a}) = \mathbf{K}\mathbf{A}(\ddot{\mathbf{q}} - \mathbf{a})\,,\end{aligned} \tag{4}$$

where $\mathbf{K}(\mathbf{q},\dot{\mathbf{q}},t) = \mathbf{M}^{1/2}(\mathbf{A}\mathbf{M}^{-1/2})^{+}$ and the superscript $+$ represents the Moore-Penrose pseudo-inverse. This solution to the GPLC (1) are known as the Udwadia-Kalaba (U-K) equations [7], which provide an analytical solution for constrained motion of mechanical systems by eliminating the Lagrange multipliers $\boldsymbol{\lambda}$ from the GPLC (1).

B. GGPLC (Higher-Order Systems)

In this section, we introduce a generalization of the GPLC that applies to systems with dynamics expressed by higher-order ODEs. In the following, we denote $\dot{\mathbf{x}} \in \mathbb{R}^N$ as a vector of the highest-order derivatives in each of a set of N ODEs. We note here that each element of $\dot{\mathbf{x}}$ can have a different order of differentiation. The following exposition simply mirrors that of Section II-A. Consider a system of N ODEs of various orders that are linear in each of their highest orders. The vector of the highest-order derivatives $\dot{\mathbf{x}}$ may be expressed in terms of unconstrained dynamics as $\mathbf{M}\dot{\mathbf{x}} = \mathbf{f}_{\rm nc}$, in which the i-th row of $\mathbf{M}$ and the i-th element of $\mathbf{f}_{\rm nc}$ may contain terms with derivatives of lower order than that in $\dot{\mathbf{x}}$.

A set of C constraints $\mathbf{g} = \mathbf{0}$, that can be functions of the states and the derivatives of the state elements up to (but not including) the corresponding orders in $\dot{\mathbf{x}}$, may be differentiated with respect to time such that the differentiated constraints are linear in $\dot{\mathbf{x}}$. To enforce a set of differentiated constraints $\mathbf{A}\dot{\mathbf{x}} = \mathbf{b}$, the constrained $\dot{\mathbf{x}}$ solves

$$\max_{\boldsymbol{\lambda}}\min_{\dot{\mathbf{x}}} \frac{1}{2}\dot{\mathbf{x}}^{\mathsf{T}}\mathbf{M}\dot{\mathbf{x}} - \dot{\mathbf{x}}^{\mathsf{T}}\mathbf{f}_{\rm nc} + \boldsymbol{\lambda}^{\mathsf{T}}(\mathbf{A}\dot{\mathbf{x}} - \mathbf{b})\ . \tag{5}$$

We call (5) the GGPLC, since it assumes a similar form as that of the GPLC (1), and $\dot{\mathbf{x}}$ denotes constrained derivatives of the highest order in each equation. The GGPLC is equivalent to minimizing the quadratic form of the difference between the true constrained highest-order derivatives and the unconstrained ones, subjected to differentiated constraints. The GGPLC leads to a KKT system for $\dot{\mathbf{x}}$ and the Lagrange multipliers $\boldsymbol{\lambda}$,

$$\begin{bmatrix}\mathbf{M} & \mathbf{A}^{\mathsf{T}}\\ \mathbf{A} & \mathbf{0}\end{bmatrix}\begin{bmatrix}\dot{\mathbf{x}}\\ \boldsymbol{\lambda}\end{bmatrix} = \begin{bmatrix}\mathbf{f}_{\rm nc}\\ \mathbf{b}\end{bmatrix}\ , \tag{6}$$

which represents the saddle point of the augmented objective (5). In the constrained equations of motion, $\mathbf{f}_{\rm c} \triangleq -\mathbf{A}^{\mathsf{T}}\boldsymbol{\lambda}$ are the actions that enforce the constraints. We note here that in this section and in the following, the variables $\mathbf{M}$, $\mathbf{f}_{\rm nc}$, $\mathbf{g}$, $\mathbf{A}$, $\mathbf{b}$, $\boldsymbol{\lambda}$, N, C, and $\mathbf{f}_{\rm c}$ correspond to the system of higher-order ODEs, whereas these variables all correspond to a system of second-order ODEs in Section II-A.

In the following application of GGPLC to the control of a quadrotor, $\mathbf{A}\dot{\mathbf{x}} = \mathbf{b}$ represents the differentiated form of path tracking constraints. $\mathbf{f}_{\rm c}$ are associated with the control thrust and moments required to bring the tracking errors to zero. In this way, Equation (6) represents a nonlinear feedback control rule to bring the quadrotor to a prescribed path. The resulting control scheme is thus nonlinear and is applied to the coupled equations of motion of a fully nonlinear quadrotor. Before presenting the unified position-attitude controller for a fully nonlinear quadroter in Section III, this section closes with a proof of the sufficient and necessary conditions for the unique solution to (6) and a description of a generalized method to stabilize a constraint $g(t)$ enforced at a differentiated level in order to recover from constraint violations that may arise from a number of exogenous factors.

C. Existence and Uniqueness of the Solution to KKT Systems

Proposition 1: The KKT system (6) is singular if and only if either (a) $\mathbf{A}^\intercal$ has a nontrivial null space, or (b) the null space of $\mathbf{M}$ intersects the null space of $\mathbf{A}$.

Proof:

- (a) $\Rightarrow$ singular KKT : If $\exists\, \boldsymbol{\lambda} \neq \mathbf{0}$ such that $\mathbf{A}^\intercal\boldsymbol{\lambda} = \mathbf{0}$, then $\dot{\mathbf{x}} = \mathbf{0}$ solves $\mathbf{M}\dot{\mathbf{x}} + \mathbf{A}^\intercal\boldsymbol{\lambda} = \mathbf{0}$. Thus, $[\mathbf{0}^\intercal\ \boldsymbol{\lambda}^\intercal]^\intercal$ is a nontrivial null space of the KKT matrix; hence, the KKT system is singular. If the constraints are linearly dependent, then any Lagrange multiplier in $\mathcal{N}(\mathbf{A}^\intercal)$ associates with constraint forces of zero.
- (b) $\Rightarrow$ singular KKT : If $\exists\, \dot{\mathbf{x}} \neq \mathbf{0}$ such that $\mathbf{M}\dot{\mathbf{x}} = \mathbf{0}$ and $\mathbf{A}\dot{\mathbf{x}} = \mathbf{0}$, then $\boldsymbol{\lambda} = \mathbf{0}$ solves both $\mathbf{M}\dot{\mathbf{x}} + \mathbf{A}^\intercal\boldsymbol{\lambda} = \mathbf{0}$ and $\mathbf{A}\dot{\mathbf{x}} = \mathbf{0}$. Hence, $[\dot{\mathbf{x}}^\intercal\ \mathbf{0}^\intercal]^\intercal$ is a nontrivial null space of the KKT matrix; thus, the KKT system is singular. If an indefinite mass matrix contains a null space that intersects with the null space of $\mathbf{A}$, then the constraint equations are not sufficient to uniquely determine $\dot{\mathbf{x}}$.
- singular KKT $\Rightarrow$ (a) or (b) : If $\exists\, [\dot{\mathbf{x}}^\intercal\ \boldsymbol{\lambda}^\intercal]^\intercal \neq \mathbf{0}$ that lies within the nontrivial null space of the KKT matrix, then $\mathbf{A}\dot{\mathbf{x}} = \mathbf{0}$, implying that either $\dot{\mathbf{x}} = \mathbf{0}$ or $\dot{\mathbf{x}} \in \mathcal{N}(\mathbf{A})$.
  - If $\dot{\mathbf{x}} = \mathbf{0}$, then $\mathbf{A}^\intercal\boldsymbol{\lambda} = \mathbf{0}$, indicating that either $\boldsymbol{\lambda} = \mathbf{0}$ or $\boldsymbol{\lambda} \in \mathcal{N}(\mathbf{A}^\intercal)$. But $[\dot{\mathbf{x}}^\intercal\ \boldsymbol{\lambda}^\intercal]^\intercal = \mathbf{0}$ is trivial. So if the KKT system is singular and $\dot{\mathbf{x}} = \mathbf{0}$, then $\exists\, \boldsymbol{\lambda} \neq \mathbf{0}$, $\boldsymbol{\lambda} \in \mathcal{N}(\mathbf{A}^\intercal)$.
  - Alternatively, if the KKT system is singular and if $\exists\, \dot{\mathbf{x}} \neq \mathbf{0}$, $\dot{\mathbf{x}} \in \mathcal{N}(\mathbf{A})$, then $\boldsymbol{\lambda}$ can be $\mathbf{0}$. Pre-multiplying ($\mathbf{M}\dot{\mathbf{x}}+\mathbf{A}^\intercal\boldsymbol{\lambda} = \mathbf{0}$) by $\dot{\mathbf{x}}^\intercal$ gives $\dot{\mathbf{x}}^\intercal\mathbf{M}\dot{\mathbf{x}} = 0$. So if the KKT system is singular and $\exists\, \dot{\mathbf{x}} \neq \mathbf{0}$, $\dot{\mathbf{x}} \in \mathcal{N}(\mathbf{A})$, then $\dot{\mathbf{x}}$ must also lie in the null space of $\mathbf{M}$.

■

D. Generalized Baumgarte's Error Stabilization (GBES)

This section describes a generalization of Baumgarte's second-order constraint error stabilization [12] to higher-order equations. Due to exogenous effects (e.g., exogenous forces, or unmodeled dynamics) and numerical integration errors, violations of constraints $\mathbf{g} = \mathbf{0}$ (e.g., tracking errors) may arise while enforcing the presumably stable dynamics

$$\mathbf{g}^{(k)} \triangleq \frac{d^k\mathbf{g}}{dt^k} = \mathbf{A}\dot{\mathbf{x}} - \mathbf{b} = \mathbf{0}\ , \tag{7}$$

where the superscript k denotes the highest differentiation order with respect to time such that the k-th time derivative of $\mathbf{g}$ is linear in the highest-order state derivatives $\dot{\mathbf{x}}$.

The intent of (7) is to enforce $\mathbf{g} = \mathbf{0}$ by enforcing $\mathbf{g}^{(k)} = \mathbf{0}$ for all time $t > 0$. However, constraint errors may accumulate even from zero initial conditions ($\mathbf{g} = \dot{\mathbf{g}} = \cdots = \mathbf{g}^{(k-1)} = \mathbf{0}$ at $t = 0$). Moreover, if (7) is nonhomogeneous, then $\mathbf{g}$ will certainly deviate from zero. The resulting constraint violations can be stabilized to zero by imposing asymptotically stable dynamics on $\mathbf{g}(t)$,

$$\frac{d^k\mathbf{g}}{dt^k} + \sum_{i=0}^{k-1}\kappa_i\frac{d^i\mathbf{g}}{dt^i} = \mathbf{0}\ , \tag{8}$$

where κ_i are called *Baumgarte coefficients* and are selected to asymptotically drive $\mathbf{g}$ to zero. Substituting (7) into (8), we obtain

$$\mathbf{A}\dot{\mathbf{x}} = \widehat{\mathbf{b}} \triangleq \mathbf{b} - \sum_{i=0}^{k-1}\kappa_i\frac{d^i\mathbf{g}}{dt^i}\ . \tag{9}$$

By prescribing the eigenvalues σ_i of (8) in terms of *natural frequencies* ω_i and *damping ratios* ζ_i,

$$\sigma_i = \zeta_i\omega_i \pm \omega_i\sqrt{\zeta_i^2 - 1}\ ,$$

the companion matrix of (8) can be computed from its eigenvalues to directly provide the Baumgarte coefficients of any differentiation order k,

$$\begin{bmatrix} 0 & 1 & 0 & \cdots & 0 \\ 0 & 0 & 1 & \cdots & 0 \\ \vdots & \vdots & & \cdots & \vdots \\ -\beta_0 & -\beta_1 & -\beta_2 & \cdots & -\beta_{k-1} \end{bmatrix} = \mathbf{V}\boldsymbol{\Lambda}\mathbf{V}^{-1}\ , \tag{10}$$

where $\boldsymbol{\Lambda}$ is a diagonal matrix of the prescribed eigenvalues σ_i, and the corresponding columns of $\mathbf{V}$ are $[1\ \sigma_i\ \sigma_i^2\ \cdots\ \sigma_i^{k-1}]^\intercal$ [13].

Enforcing the stabilized differentiated constraints (9) instead of (7) in (6), we have

$$\begin{bmatrix} \mathbf{M} & \mathbf{A}^\intercal \\ \mathbf{A} & \mathbf{0} \end{bmatrix}\begin{bmatrix} \dot{\mathbf{x}} \\ \boldsymbol{\lambda} \end{bmatrix} = \begin{bmatrix} \mathbf{f}_{\text{nc}} \\ \widehat{\mathbf{b}} \end{bmatrix}\ , \tag{11}$$

which we term the GGPLC KKT system with constraint stabilization.

Importantly, since the eigenvalues of (8) (a linear ODE) are user-prescribed via (10), any constraint violation is guaranteed to converge to zero with the dynamics specified by ω_i and ζ_i.

It is worthwhile to note that our GGPLC is more flexible than the U-K equations in that the GGPLC method (a) can handle systems of higher-order dynamics such as a quadrotor, while U-K methods can only handle second-order dynamical systems; (b) can asymptotically drive inadmissible initial states and constraint violations to zero; (c) can demonstrate, through Lagrange multipliers, how the contribution of each constraint couples to the total control actions; and (d) is computationally efficient as it only involves solving a KKT system (a matrix equation) at any instant of time; no pseudo-inverse computations or convergent iterative methods are involved.

III. Unified Control for Constrained Fully Nonlinear Quadrotor Dynamics

A. Fully Nonlinear Quadrotor Dynamics

A quadrotor has six degrees of freedom and four control inputs generated from the four spinning propellers. The inertial frame is fixed to the ground with positive Z axis pointing upwards, while the body-fixed frame coincides with the principle axes of the quadrotor with thrust force acting along positive body Z axis, which is perpendicular to the quadrotor plane (body X-Y plane). The rotation matrix from the body frame to the inertial frame is described by ZYX

Euler angles, roll $\phi \in [-\pi, \pi]$, pitch $\theta \in (-\pi/2, \pi/2)$, and yaw $\psi \in [-\pi, \pi]$:

$$\mathbf{R} \triangleq \begin{bmatrix} \mathbf{x}_{\mathrm{B}}^{\mathsf{T}} \\ \mathbf{y}_{\mathrm{B}}^{\mathsf{T}} \\ \mathbf{z}_{\mathrm{B}}^{\mathsf{T}} \end{bmatrix}^{\mathsf{T}} = \begin{bmatrix} \mathrm{c}\psi\mathrm{c}\theta & \mathrm{c}\psi\mathrm{s}\theta\mathrm{s}\phi - \mathrm{s}\psi\mathrm{c}\phi & \mathrm{c}\psi\mathrm{s}\theta\mathrm{c}\phi + \mathrm{s}\psi\mathrm{s}\phi \\ \mathrm{s}\psi\mathrm{c}\theta & \mathrm{s}\psi\mathrm{s}\theta\mathrm{s}\phi + \mathrm{c}\psi\mathrm{c}\phi & \mathrm{s}\psi\mathrm{s}\theta\mathrm{c}\phi - \mathrm{c}\psi\mathrm{s}\phi \\ -\mathrm{s}\theta & \mathrm{c}\theta\mathrm{s}\phi & \mathrm{c}\theta\mathrm{c}\phi \end{bmatrix}, \tag{12}$$

where s and c are shorthanded for sine and cosine, respectively. The Euler angle rates $\dot{\mathbf{\Theta}}_{\mathrm{E}}$ are calculated by

$$\dot{\mathbf{\Theta}}_{\mathrm{E}} = \begin{bmatrix} \dot{\phi} \\ \dot{\theta} \\ \dot{\psi} \end{bmatrix} = \mathbf{E}\,\boldsymbol{\omega}_{\mathrm{B}} = \begin{bmatrix} 1 & \mathrm{s}\phi\,\mathrm{t}\theta & \mathrm{c}\phi\,\mathrm{t}\theta \\ 0 & \mathrm{c}\phi & -\mathrm{s}\phi \\ 0 & \mathrm{s}\phi/\mathrm{c}\theta & \mathrm{c}\phi/\mathrm{c}\theta \end{bmatrix} \boldsymbol{\omega}_{\mathrm{B}}\ , \tag{13}$$

where t is shorthanded for tangent, and $\boldsymbol{\omega}_{\mathrm{B}} = [p\ q\ r]^{\mathsf{T}} \in \mathbb{R}^3$ are the angular velocities expressed in the body frame.

We model a quadrotor as a rigid body and describe its dynamics by the Newton-Euler equations [14], [15],

$$m\,\ddot{\mathbf{p}}_{\mathrm{I}} = f_{\mathrm{t}}\mathbf{R}\mathbf{e}_3 - G\mathbf{e}_3 = f_{\mathrm{t}}\mathbf{z}_{\mathrm{B}} - G\mathbf{e}_3\ , \tag{14}$$

$$\mathbf{J}\,\dot{\boldsymbol{\omega}}_{\mathrm{B}} + \boldsymbol{\omega}_{\mathrm{B}} \times (\mathbf{J}\,\boldsymbol{\omega}_{\mathrm{B}}) = \boldsymbol{\tau}_{\mathbf{B}}\ , \tag{15}$$

where m is the total mass, G is the magnitude of the gravity, $\mathbf{p}_{\mathrm{I}} = [x\ y\ z]^{\mathsf{T}} \in \mathbb{R}^3$ are the position coordinates of the center of mass expressed in the inertial frame, $\mathbf{e}_3 = [0\ 0\ 1]^{\mathsf{T}}$, the overdot denotes the differentiation with respect to time, f_{t} is the magnitude of the total thrust force acting in the body Z axis, $\mathbf{J} = \mathrm{diag}(I_x, I_y, I_z) \in \mathbb{R}^{3\times3}$ is a diagonal matrix of the principal moments of inertia of the quadrotor, $\times$ denotes the cross product operation of two vectors, and $\boldsymbol{\tau}_{\mathrm{B}} = [\tau_1\ \tau_2\ \tau_3]^{\mathsf{T}} \in \mathbb{R}^3$ contains the control torques expressed in the body frame. Note that a bijection exists between $[f_{\mathrm{t}}\ \boldsymbol{\tau}_{\mathrm{B}}^{\mathsf{T}}]$ and Ω_i^2, $i = 1, 2, 3, 4$, the squared spinning speeds of four propellers [14]. In this study, we adopt $[f_{\mathrm{t}}\ \boldsymbol{\tau}_{\mathrm{B}}^{\mathsf{T}}]$ as the inputs to quadrotor dynamics, as we can always recover Ω_i as true inputs once we have $[f_{\mathrm{t}}\ \boldsymbol{\tau}_{\mathrm{B}}^{\mathsf{T}}]$ in real world implementations.

By differentiating (14), we have respectively the jerk and snap dynamics expressed in the inertial frame as

$$m\dddot{\mathbf{p}}_{\mathrm{I}} = \dot{f}_{\mathrm{t}}\mathbf{z}_{\mathrm{B}} + f_{\mathrm{t}}\mathbf{R}\hat{\boldsymbol{\omega}}_{\mathrm{B}}\mathbf{e}_3\,, \tag{16}$$

$$m\ddddot{\mathbf{p}}_{\mathrm{I}} = \ddot{f}_{\mathrm{t}}\mathbf{z}_{\mathrm{B}} + 2\dot{f}_{\mathrm{t}}\mathbf{R}\hat{\boldsymbol{\omega}}_{\mathrm{B}}\mathbf{e}_3 + f_{\mathrm{t}}(\mathbf{R}\hat{\boldsymbol{\omega}}_{\mathrm{B}}^2\mathbf{e}_3 + \mathbf{R}\dot{\hat{\boldsymbol{\omega}}}_{\mathrm{B}}\mathbf{e}_3)\,, \tag{17}$$

where $\hat{\boldsymbol{\omega}}_{\mathrm{B}}$ denotes the skew-symmetric matrix of $\boldsymbol{\omega}_{\mathrm{B}}$, and

$$\dot{\mathbf{R}} = \mathbf{R}\hat{\boldsymbol{\omega}}_{\mathrm{B}} = \begin{bmatrix} \mathbf{x}_{\mathrm{B}}^{\mathsf{T}} \\ \mathbf{y}_{\mathrm{B}}^{\mathsf{T}} \\ \mathbf{z}_{\mathrm{B}}^{\mathsf{T}} \end{bmatrix}^{\mathsf{T}} \begin{bmatrix} 0 & -r & q \\ r & 0 & -p \\ -q & p & 0 \end{bmatrix}\ . \tag{18}$$

Equation (17) shows that the rotational dynamics is coupled with the translational dynamics at the levels of snap and angular acceleration. Therefore, the equations of motion of a fully nonlinear quadrotor can be expressed by Equations (17) and (15)

$$\begin{bmatrix} m\mathbf{I}_3 & \mathbf{M}_{12} \\ \mathbf{0}_{3\times3} & \mathbf{J} \end{bmatrix} \begin{bmatrix} \ddddot{\mathbf{p}}_{\mathrm{I}} \\ \dot{\boldsymbol{\omega}}_{\mathrm{B}} \end{bmatrix} = \begin{bmatrix} \ddot{f}_{\mathrm{t}}\mathbf{z}_{\mathrm{B}} + 2\dot{f}_{\mathrm{t}}\mathbf{R}\hat{\boldsymbol{\omega}}_{\mathrm{B}}\mathbf{e}_3 + f_{\mathrm{t}}\mathbf{R}\hat{\boldsymbol{\omega}}_{\mathrm{B}}^2\mathbf{e}_3 \\ \boldsymbol{\tau}_{\mathrm{B}} - \hat{\boldsymbol{\omega}}_{\mathrm{B}}\mathbf{J}\boldsymbol{\omega}_{\mathrm{B}} \end{bmatrix}, \tag{19}$$

where the term

$$\mathbf{M}_{12}\dot{\boldsymbol{\omega}}_{\mathrm{B}} \triangleq \begin{bmatrix} f_{\mathrm{t}}\mathbf{y}_{\mathrm{B}} & -f_{\mathrm{t}}\mathbf{x}_{\mathrm{B}} & \mathbf{0} \end{bmatrix} \begin{bmatrix} \dot{p} & \dot{q} & \dot{r} \end{bmatrix}^{\mathsf{T}} = -f_{\mathrm{t}}\mathbf{R}\dot{\hat{\boldsymbol{\omega}}}_{\mathrm{B}}\mathbf{e}_3$$

achieves the coupling of the rotational dynamics with the translational dynamics.

In (19), the command controls due to active constraints are $\ddot{f}_{\mathrm{t}}$ and $\boldsymbol{\tau}_{\mathrm{B}}$, and f_{t} and $\dot{f}_{\mathrm{t}}$ are treated as states. $f_{\mathrm{t}}\mathbf{R}\hat{\boldsymbol{\omega}}_{\mathrm{B}}^2\mathbf{e}_3$ may be regarded as a *centrifugal* term, $2\dot{f}_{\mathrm{t}}\mathbf{R}\hat{\boldsymbol{\omega}}_{\mathrm{B}}\mathbf{e}_3$ may be regarded as a *Coriolis* term, and $\ddot{f}_{\mathrm{t}}\mathbf{z}_{\mathrm{B}}$ may be considered as the "*generalized actuation force*" expressed in the inertial frame as in Newton's Second Law. Note that (19) is underactuated since no control is exerted on $\dddot{x}$ or $\dddot{y}$.

Due to the inherent full coupling of the dynamics in (19), we eliminate $\dot{p}$ and $\dot{q}$ from (19) by substituting $\dot{p} = [\tau_1 - (I_z - I_y)qr]/I_x$ and $\dot{q} = [\tau_2 - (I_x - I_z)pr]/I_y$ from (15) into (19) to obtain

$$\begin{bmatrix} m\mathbf{I}_3 & \mathbf{0}_{3\times1} \\ \mathbf{0}_{1\times3} & I_z \end{bmatrix} \begin{bmatrix} \ddddot{\mathbf{p}}_{\mathrm{I}} \\ \dddot{r} \end{bmatrix} = \begin{bmatrix} \mathbf{f}_{\mathrm{ut}} \\ (I_x - I_y)pq \end{bmatrix} + \begin{bmatrix} \mathbf{z}_{\mathrm{B}} & -f_{\mathrm{t}}\mathbf{y}_{\mathrm{B}}/I_x & f_{\mathrm{t}}\mathbf{x}_{\mathrm{B}}/I_y & \mathbf{0}_{3\times1} \\ 0 & 0 & 0 & 1 \end{bmatrix} \begin{bmatrix} \ddot{f}_{\mathrm{t}} \\ \boldsymbol{\tau}_{\mathrm{B}} \end{bmatrix}\ , \tag{20}$$

where $\mathbf{f}_{\mathrm{ut}} = [(I_y + I_z - I_x)f_{\mathrm{t}}pr/I_y + 2\dot{f}_{\mathrm{t}}q]\mathbf{x}_{\mathrm{B}} + [(I_x + I_z - I_y)f_{\mathrm{t}}qr/I_x - 2\dot{f}_{\mathrm{t}}p]\mathbf{y}_{\mathrm{B}} - [f_{\mathrm{t}}(p^2 + q^2)]\mathbf{z}_{\mathrm{B}}$. Equation (20) can be compactly written as $\mathbf{M}\dot{\mathbf{x}} = \mathbf{f}_{\mathrm{nc}} + \mathbf{B}\mathbf{u}$. It is evident from (20) that the four highest-order state derivatives, $\ddddot{\mathbf{p}}_{\mathrm{I}}$ and $\dddot{r}$, are controlled independently by four command inputs, $\ddot{f}_{\mathrm{t}}$ and $\boldsymbol{\tau}_{\mathrm{B}}$. As long as the drone is constrained from free falling, f_{t} will be nonzero for all time. The quadrotor thus becomes a fully actuated system in a reduced configuration space, with the input influence matrix $\mathbf{B} \in \mathbb{R}^{4\times4}$ being full rank.

B. Constraint Formulation

We want the quadrotor to track a reference trajectory $\mathbf{p}_{\mathrm{r}}(t) = [\bar{x}(t)\ \bar{y}(t)\ \bar{z}(t)]^{\mathsf{T}} \in \mathbb{R}^3$ as accurate as possible. We formulate tracking objective as three decomposed equality constraints $\mathbf{g}_{\mathrm{t}} \triangleq \Delta\mathbf{p}_{\mathrm{I}} = [x - \bar{x}\ \ y - \bar{y}\ \ z - \bar{z}]^{\mathsf{T}} = \mathbf{0}_{3\times1}$ whose first-, second-, third-, and fourth-order time derivatives are respectively $\dot{\mathbf{g}}_{\mathrm{t}} = \Delta\dot{\mathbf{p}}_{\mathrm{I}}$, $\ddot{\mathbf{g}}_{\mathrm{t}} = \Delta\ddot{\mathbf{p}}_{\mathrm{I}}$, $\dddot{\mathbf{g}}_{\mathrm{t}} = \Delta\dddot{\mathbf{p}}_{\mathrm{I}}$, and $\ddddot{\mathbf{g}}_{\mathrm{t}} = \Delta\ddddot{\mathbf{p}}_{\mathrm{I}}$. Hence, the tracking constraints integrated with the generalized error stabilization scheme become

$$\ddddot{\mathbf{p}}_{\mathrm{I}} = \ddddot{\mathbf{p}}_{\mathrm{r}} - \kappa_3\Delta\dddot{\mathbf{p}}_{\mathrm{I}} - \kappa_2\Delta\ddot{\mathbf{p}}_{\mathrm{I}} - \kappa_1\Delta\dot{\mathbf{p}}_{\mathrm{I}} - \kappa_0\Delta\mathbf{p}_{\mathrm{I}} = \widehat{\mathbf{b}}\,, \tag{21}$$

which is incorporated into (11) as $\mathbf{A}\dot{\mathbf{x}} = \widehat{\mathbf{b}}$.

C. Selection of Baumgarte Coefficients

The Baumgarte coefficients κ_i, $i = 0, 1, 2, 3$, in (21) are the only user-defined control parameters in this unified position-attitude controller for a fully nonlinear quadrotor.

During the natural evolution of constrained system dynamics, the onset of an active constraint g leads to initial conditions for zero g_{in} and generically nonzero (problem dependent) $\dot{g}_{\mathrm{in}}$, $\ddot{g}_{\mathrm{in}}$, and $\dddot{g}_{\mathrm{in}}$, with faster dynamics subject to a generally higher initial value. Thus, an optimization problem that minimizes the peak constraint position subject to zero initial constraint position and nonzero initial constraint velocity, acceleration, and jerk can be posed as

$$\begin{aligned} &\min_{\omega_i, \zeta_i} \max_{t}\ g(\mathbf{q}, t) \qquad g_{\mathrm{in}} = 0,\ \dot{g}_{\mathrm{in}} = 1\,,\ \ddot{g}_{\mathrm{in}} = 2\,,\ \dddot{g}_{\mathrm{in}} = 3 \\ &\text{s.t. } |\sigma_i|_{\min} \le |\sigma_i| \le |\sigma_i|_{\max} \quad \text{and} \quad \zeta_{i,\min} \le \zeta_i \le \zeta_{i,\max} \end{aligned} \tag{22}$$

to find an optimal set of Baumgarte coefficients, where the frequency and damping of the constraint dynamics are

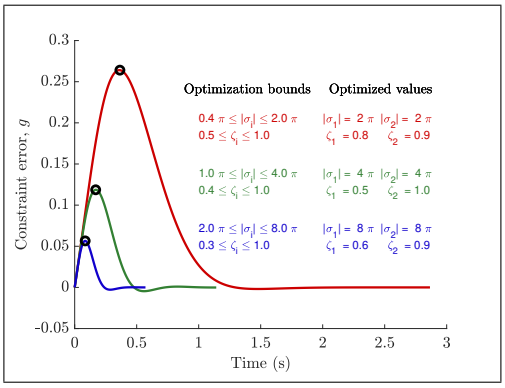

Fig. 1. Representative convergence of constraint violation to zero via a GBES parameterized by natural frequencies ω_i and damping ratios ζ_i.

constrained to lie within user-specified ranges. So doing, this optimization generally results in optimized damping ratios lying within the specified range and $|\sigma_i|_{\text{opt}} = |\sigma_i|_{\max}$.

D. GGPLC KKT System with Constraint Stabilization

With the constrained quadrotor dynamics (20) and the constraint dynamics (21), the system (11) for a fully nonlinear quadrotor tracking problem becomes

$$\begin{bmatrix} m\mathbf{I}_3 & \mathbf{0}_{3\times1} & \mathbf{I}_3 \\ \mathbf{0}_{1\times3} & I_z & \mathbf{0}_{1\times3} \\ \mathbf{I}_3 & \mathbf{0}_{3\times1} & \mathbf{0}_{3\times3} \end{bmatrix} \begin{bmatrix} \dddot{\mathbf{p}}_{\text{I}} \\ \dot{r} \\ \boldsymbol{\lambda} \end{bmatrix} = \begin{bmatrix} \mathbf{f}_{\text{nc}} \\ \hat{\mathbf{b}} \end{bmatrix}, \tag{23}$$

where $\mathbf{I}$ denotes an identity matrix. Since $\mathbf{A} = [\mathbf{I}_3 \ \mathbf{0}_{3\times1}]$ is always full rank, Equation (23) always has a unique solution according to Proposition 1. $-\mathbf{A}^{\text{T}}\boldsymbol{\lambda} = \mathbf{B}\mathbf{u}$ provides the control actions that enforce tracking along three inertial axes. Since $\mathbf{B}$ is full rank in all scenarios except the unconstrained free falling, the control actions can be solved by $\mathbf{u} = -\mathbf{B}^{-1}\mathbf{A}^{\text{T}}\boldsymbol{\lambda}$. Then, $\dot{p}$ and $\dot{q}$ can be obtained by substituting τ_1 and τ_2 into (15). In a real world implementation, the actual control inputs provided by the four rotors are f_{t} and $\boldsymbol{\tau}_{\text{B}}$, where f_{t} is a state and is equal to double integrating $\ddot{f}_{\text{t}}$ that is solved from (23).

Constant-step fourth-order Runge-Kutta method is used for numerical integration, where there are in total 20 states: $\mathbf{p}_{\text{I}}$, $\dot{\mathbf{p}}_{\text{I}}$, $\ddot{\mathbf{p}}_{\text{I}}$, $\dddot{\mathbf{p}}_{\text{I}}$, $\boldsymbol{\Theta}_{\text{E}}$, $\boldsymbol{\omega}_{\text{B}}$, f_{t}, and $\dot{f}_{\text{t}}$.

IV. NUMERICAL RESULTS

Based on the proposed method, we control a fully nonlinear quadrotor to track a reference path: $\bar{x}(t) = 1.2t\cos(2\pi t/5)$, $\bar{y}(t) = 1.2t\sin(2\pi t/5)$, $\bar{z}(t) = t$, $\forall t \in [0, 10]$ s; for $t > 10$ s, the reference path remains stationary at $[\bar{x}(10)\ \bar{y}(10)\ \bar{z}(10)]^{\text{T}}$. The numerical simulation is conducted in MATLAB on a Windows laptop with a 2.50 GHz Intel i5-7200U CPU and 8 GB memory. The parameters used in this study are: $m = 10$ kg, $g = 9.8$ kg/m^2, $2I_x = 2I_y = I_z = 2$ kg·m^2, $\kappa_0 = 1558.5$, $\kappa_1 = 849.89$, $\kappa_2 = 194.53$, $\kappa_3 = 21.528$, and the constant time step $\Delta t = 0.005$ s. In practice, the Baumgarte coefficients may be selected in relation to actuator bandwidth and force capacity. In this example, the Baumgarte coefficients result from solving the optimization problem (22) with bounds $0.4\pi \le |\sigma_i| \le 2\pi$ and $0.5 \le \zeta_i \le 1.0$, resulting in $|\sigma_1| = |\sigma_2| = 2\pi$ rad/s, $\zeta_1 = 0.8$, and $\zeta_2 = 0.9$, as shown in Fig. 1. The quadrotor starts with all zero states except the initial position at $[-5\ 5\ 0]^{\text{T}}$ in the inertial frame and the initial thrust $f_{\text{t}} = mg = G$.

The trajectories of the reference point and the drone are presented in Fig. 2. Snapshots of the body-fixed frame are also shown along the evolution of dynamics. We can observe that the thrust axis (i.e., positive body Z axis, the blue line in Fig. 2) tilts towards the reference point from the offset initial position. After $t = 2$ s, the drone tracks the reference with thrust axis pointing inwards the conical spiral, counterbalancing the gravity and centrifugal force. Immediately after $t = 10$ s, the quadrotor is subjected to an overshoot due to its momentum and an abrupt change in the reference velocities (from $[\dot{\bar{x}}\ \dot{\bar{y}}\ \dot{\bar{z}}] = [1.2\ 15.08\ 1]$ m/s at $t = 10$ s to $[\dot{\bar{x}}\ \dot{\bar{y}}\ \dot{\bar{z}}] = [0\ 0\ 0]$ at $t > 10$ s). During the overshoot, the drone (a) first decelerates to zero speed, then (b) accelerates and (c) decelerates towards the stationary reference point, and finally (d) stabilizes at the stationary reference point in horizontal hover. The thrust axis tilts towards the reference point in (a) and (b) and tilts away from the reference point in (c). The good tracking performance of the proposed control can also be viewed from the motion time series of the reference point and the quadrotor in Fig. 3. The corresponding 3-D animation is available online. [1]

Since the row in $\mathbf{A}^{\text{T}}$ that corresponds to $\dot{r}$ in (23) is $\mathbf{0}_{1\times3}$, τ_3 in $-\mathbf{B}^{-1}\mathbf{A}^{\text{T}}\boldsymbol{\lambda}$ is zero for all time, as shown in Fig. 4. Thus, r is always the initial value (zero), as shown in Fig. 5. Since we do not constrain the quadrotor to track a reference yaw angle, the body X-Y plane is consistently yawing by responding to the natural evolution of the constrained fully nonlinear quadrotor dynamics. When the tracking errors are reasonably small (both when tracking the spiral and when stabilized at horizontal hover), no control torques about body X and Y axes are applied, which is shown in Fig. 4.

The elapsed real time calculation for obtaining control actions considers the time accumulated over the 20-s simulation window that is spent on constructing and solving the GGPLC KKT system (23) and on computing the control actions $\mathbf{u}$. Then, the computation time per iteration is obtained by dividing the total accumulative elapsed real time by the total number of integration steps. In this study, the computation time per iteration is 3.98×10^{-5} s, demonstrating the computational efficiency and thus the promise of real world applications of our method.

V. CONTRIBUTIONS AND FUTURE WORK

We have developed an efficient, novel, nonlinear control architecture for higher-order constrained dynamical systems and applied it to the tracking control of a fully nonlinear quadrotor. The proposed method is based on a generalization of GPLC combined with a generalized constraint error stabilization. To the best of our knowledge, our work is (a) the first generalization and application of GPLC to control

[1] https://youtu.be/-1QB2EVS2fQ

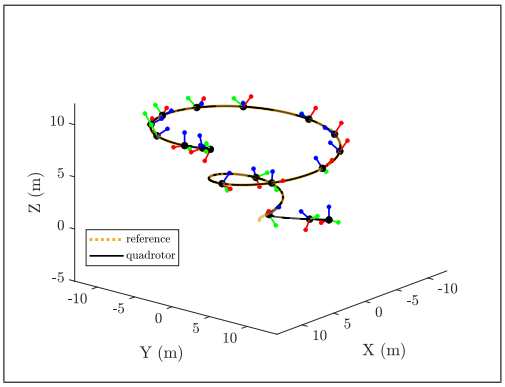

Fig. 2. A fully nonlinear quadrotor tracks a reference trajectory (first a conical spiral, then at rest at the end position) with snapshots of the drone's body frame along dynamics evolution. The red, green, and blue lines denote the X, Y, and Z axes of the body frame, respectively. The control thrust vector acts along the positive body Z axis.

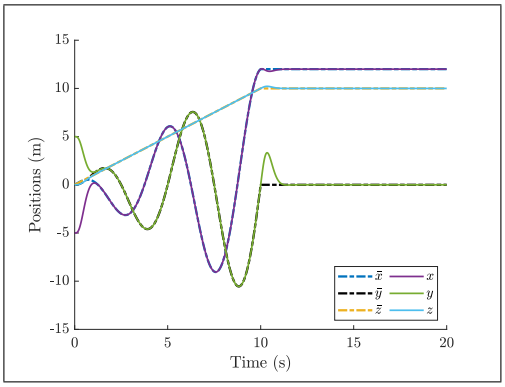

Fig. 3. Motion time series of the quadrotor and the reference path.

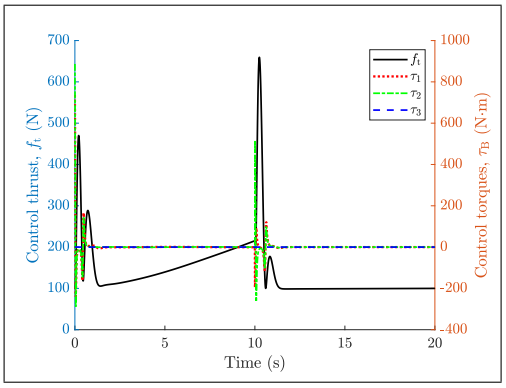

Fig. 4. Time series of the control thrust and control torques expressed in the body frame.

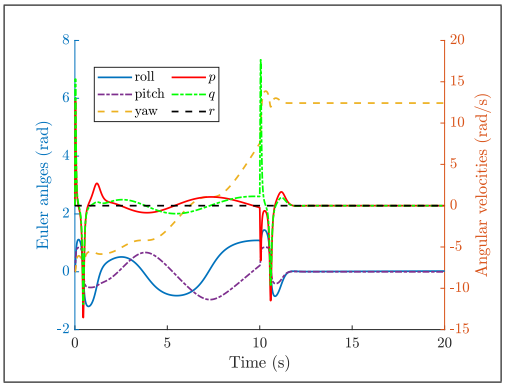

Fig. 5. Time series of Euler angles and angular velocities.

higher-order constrained dynamical systems, (b) the first generalization of Baumgarte's second-order error stabilization to higher-order constraint dynamics, and (c) the first unified one-step position-attitude control for a quadrotor that is due purely to its constrained *fully nonlinear* dynamics and that possesses a globally optimal solution.

Along this promising line of research, the proposed control method can be further developed to handle scenarios involving: linearly dependent constraints, actuator delay, saturation, modeling uncertainties, exogenous disturbances, obstacle avoidance, collision avoidance, quadrotor team coordination, and decentralized architectures. In addition, our control algorithm is promising for real world experiments, thanks to its structure simplicity and computation efficiency.

REFERENCES

[1] B. J. Emran and H. Najjaran, "A review of quadrotor: An underactuated mechanical system," *Annu. Rev. Contr.*, vol. 46, pp. 165–180, 2018.

[2] T. P. Nascimento and M. Saska, "Position and attitude control of multi-rotor aerial vehicles: A survey," *Annu. Rev. Contr.*, vol. 48, pp. 129–146, 2019.

[3] J. Kim, M.-S. Kang, and S. Park, "Accurate modeling and robust hovering control for a quad–rotor VTOL aircraft," *J. Intell. Robot. Syst.*, vol. 57, no. 1, pp. 9–26, 2010.

[4] A. Murilo and R. V. Lopes, "Unified NMPC framework for attitude and position control for a VTOL UAV," *Proc. Inst. Mech. Eng. I*, vol. 233, no. 7, pp. 889–903, 2019.

[5] C. De Crousaz, F. Farshidian, M. Neunert, and J. Buchli, "Unified motion control for dynamic quadrotor maneuvers demonstrated on slung load and rotor failure tasks," in *Proc. IEEE Int. Conf. Robot. Autom.*, 2015, pp. 2223–2229.

[6] M. Neunert, C. De Crousaz, F. Furrer, M. Kamel, F. Farshidian, R. Siegwart, and J. Buchli, "Fast nonlinear model predictive control for unified trajectory optimization and tracking," in *Proc. IEEE Int. Conf. Robot. Autom.*, 2016, pp. 1398–1404.

[7] F. E. Udwadia and R. E. Kalaba, "A new perspective on constrained motion," *Proc.: Math. Phys. Sci.*, vol. 439, no. 1906, pp. 407–410, 1992.

[8] C. F. Gauß, "Über ein neues allgemeines grundgesetz der mechanik." *J. für die Reine und Angew. Math.*, vol. 4, pp. 232–235, 1829.

[9] H. Cho and F. E. Udwadia, "Explicit solution to the full nonlinear problem for satellite formation-keeping," *Acta Astronaut.*, vol. 67, no. 3-4, pp. 369–387, 2010.

[10] B. Shirani, M. Najafi, and I. Izadi, "Cooperative load transportation using multiple UAVs," *Aerosp. Sci. Technol.*, vol. 84, pp. 158–169, 2019.

[11] B. Zhang and H. P. Gavin, "Gauss's principle with inequality constraints for multi-agent navigation and control," *IEEE Trans. Automat. Contr.*, accepted. [Online]. Available: http://dx.doi.org/10.1109/TAC.2021.3059677

[12] J. Baumgarte, "Stabilization of constraints and integrals of motion in dynamical systems," *Comput. Methods in Appl. Mech. Eng.*, vol. 1, no. 1, pp. 1–16, 1972.

[13] D. S. Bernstein, *Scalar, Vector, and Matrix Mathematics: Theory, Facts, and Formulas-Revised and Expanded Edition.* Princeton university press, 2018.

[14] D. Mellinger and V. Kumar, "Minimum snap trajectory generation and control for quadrotors," in *Proc. IEEE Int. Conf. Robot. Autom.*, 2011, pp. 2520–2525.

[15] T. Lee, M. Leoky, and N. H. McClamroch, "Geometric tracking control of a quadrotor UAV on SE(3)," in *Proc. 49th IEEE Conf. Decis. Control*, 2010, pp. 5420–5425.